

PROJECTIVE IMAGE ALIGNMENT BY USING ECC MAXIMIZATION

Georgios D. Evangelidis and Emmanouil Z. Psarakis

Department of Computer Engineering and Informatics, University of Patras, 26500 Rio, Patras, Greece

Keywords: Image alignment, image registration, motion estimation, parametric motion, image matching, mosaic construction, gradient methods, correlation coefficient.

Abstract: Nonlinear projective transformation provides the exact number of desired parameters to account for all possible camera motions thus making its use in problems where the objective is the alignment of two or more image profiles to be considered as a natural choice. Moreover, the ability of an alignment algorithm to quickly and accurately estimate the parameter values of the geometric transformation even in cases of over-modelling of the warping process constitutes a basic requirement to many computer vision applications. In this paper the appropriateness of the Enhanced Correlation Coefficient (ECC) function as a performance criterion in the projective image registration problem is investigated. Since this measure is a highly nonlinear function of the warp parameters, its maximization is achieved by using an iterative technique. The main theoretical results concerning the nonlinear optimization problem and an efficient approximation leading to an optimal closed form solution (per iteration) are presented. The performance of the iterative algorithm is compared against the well known Lucas-Kanade algorithm with the help of a series of experiments involving strong or weak geometric deformations, ideal and noisy conditions and even over-modelling of the warping process. In all cases ECC based algorithm exhibits a better behavior in speed, as well as in the probability of convergence as compared to the Lucas-Kanade scheme.

1 INTRODUCTION

The image alignment problem can be seen as a mapping between the coordinates systems of two or more images, therefore the first step towards its solution is the choice of an appropriate geometric transformation that adequately models this mapping. Eight-parameters projective transformation provides the exact number of desired parameters to account for all possible camera motions, therefore its use in the parametric image alignment problem is considered as the most natural choice. This class of transformations and in particular several of its subclasses as affine, similitude transformations and pure translation have been in the center of attention in many applications (Fuh and Maragos, 1991; Gleicher, 1997; Hager and Belhumeur, 1998; Baker and Matthews, 2004; Szeliski, 2006).

Once the parametric transformation has been defined the alignment problem reduces into a parameter estimation problem. Therefore, the second critical step towards its solution is the definition of an appro-

appropriate objective function. Most existing techniques adopt measures which are l_p based norms of the error between either the whole image profiles (*pixel-based techniques*) or specific feature of image profiles (*feature-based techniques*) (Szeliski, 2005), with the l_2 norm being by far the most widely used (Lucas and Kanade, 1981; Anandan, 1989; Fuh and Maragos, 1991; Hager and Belhumeur, 1998; Shum and Szeliski, 2000; Baker and Matthews, 2004; Szeliski, 2006; Evangelidis and Psarakis, 2007).

Independently of the used measure, for the optimum estimation of the parameters most of the existing *pixel-based techniques* require the use of gradient based iterative optimization techniques. However, the choice of the measure, the form of the alternative expression that approximates the original nonlinear objective function in each iteration of the alignment algorithm and the number of the parameters to be estimated, affect its accuracy, speed and probability of convergency as well as its robustness against possible photometric distortions.

In this paper the appropriateness of Enhanced Correlation Coefficient (Evangelidis and Psarakis, 2007) as a performance criterion for the eight-parameters nonlinear projective registration problem is investigated. Since the measure is a highly nonlinear function of the warp parameters, its maximization is achieved by using an iterative technique. The main theoretical results concerning the nonlinear optimization problem and an efficient approximation that leads to an optimal closed form solution (per iteration) are presented. The performance of the algorithm is compared against the well known Lucas-Kanade algorithm with the help of a series of experiments. In all experiments the eight-parameters mentioned transformation is used to model the warping process. Two sets of experiments are conducted. That differentiates these sets is the class of the transformations we use to create the image profiles. Specifically, in the first set of experiments the reference image profiles are created by using a nonlinear projective transformation (minimal case). In the second set of experiments (over-modelling case), in order to quantify the impact of mismatches between the actual motion model and that used by the algorithms, reference image profiles are created by using affine transformations and the behavior of the iterative algorithms under the influence of over modelling is examined.

The remainder of this paper is organized as follows. In Section 2, we formulate the parametric image alignment problem. In Section 3, the ECC based nonlinear optimization problem is defined; the iterative alignment algorithm and a closed form optimal solution of the basic (per iteration) optimization problem are given. In Section 4, we apply the ECC based technique in a number of experiments and a detailed comparison of our algorithm with the Lucas-Kanade alignment scheme is provided. Finally, Section 5 contains our conclusions.

2 PROBLEM FORMULATION

In this section we formulate the problem of alignment of two image profiles. Let us assume that a *reference* image $I_r(\mathbf{x})$ and a *warped* image $I_w(\mathbf{x}')$ are given, where $\mathbf{x} = [x, y]$ and $\mathbf{x}' = [x', y']$ denote image coordinates. Suppose also that we are given a set of coordinates $S = \{\mathbf{x}_i | i = 1, \dots, K\}$ in the reference image, which is called *target area*. Then, the alignment problem consists in finding the corresponding coordinate set in the warped image.

By considering that a transformation model $T(\mathbf{x}; \mathbf{p})$ where $\mathbf{p} = (p_1, p_2, \dots, p_N)^t$ is a vector of unknown parameters is given, the alignment problem is

reduced to the problem of estimating the parameter vector \mathbf{p} such that

$$I_r(\mathbf{x}) = \Psi(I_w(T(\mathbf{x}; \mathbf{p})); \alpha), \mathbf{x} \in S, \quad (1)$$

where transformation $\Psi(I, \alpha)$ which is parameterized by a vector α , accounts for possible photometric distortions that violate the brightness constancy assumption, a case which arises in real applications due to different viewing directions and/or different illumination conditions.

The goal of most existing algorithms is the minimization of the dissimilarity of the two image profiles, providing the optimum parameter values. Dissimilarity is usually expressed through an objective function $E(\mathbf{p}, \alpha)$ which involves the l_p norm of the intensity residual of the image profiles. A typical minimization problem has the following form

$$\min_{\mathbf{p}, \alpha} E(\mathbf{p}, \alpha) = \min_{\mathbf{p}, \alpha} \sum_{\mathbf{x} \in S} |I_r(\mathbf{x}) - \Psi(I_w(T(\mathbf{x}; \mathbf{p})), \alpha)|^p. \quad (2)$$

Solving the above defined problem is not a simple task because of the nonlinearity involved in the correspondence part. Computational complexity and estimation quality of existing schemes depends on the specific l_p norm and the models used for warping and photometric distortion. As far as the norm power p is concerned most methods use $p = 2$ (Euclidean norm). This will also be the case in the approach we briefly present in the next section.

3 THE ALIGNMENT ALGORITHM

It is more convenient at this point to define the *reference vector* \mathbf{i}_r and the *warped vector* $\mathbf{i}_w(\mathbf{p})$ as follows

$$\mathbf{i}_r = \begin{bmatrix} I_r(\mathbf{x}_1) \\ I_r(\mathbf{x}_2) \\ \vdots \\ I_r(\mathbf{x}_K) \end{bmatrix}, \quad \mathbf{i}_w(\mathbf{p}) = \begin{bmatrix} I_w(T(\mathbf{x}_1; \mathbf{p})) \\ I_w(T(\mathbf{x}_2; \mathbf{p})) \\ \vdots \\ I_w(T(\mathbf{x}_K; \mathbf{p})) \end{bmatrix} \quad (3)$$

and denote by $\bar{\mathbf{i}}_r$ and $\bar{\mathbf{i}}_w(\mathbf{p})$ the zero-mean versions of the reference and warped vector respectively. We then propose the following l_2 based criterion to quantify the performance of the warping transformation with parameters \mathbf{p}

$$E_{ECC}(\mathbf{p}) = \left\| \frac{\bar{\mathbf{i}}_r}{\|\bar{\mathbf{i}}_r\|} - \frac{\bar{\mathbf{i}}_w(\mathbf{p})}{\|\bar{\mathbf{i}}_w(\mathbf{p})\|} \right\|^2, \quad (4)$$

where $\|\cdot\|$ denotes the usual Euclidean norm.

It is clear from (4) that this criterion is invariant to possibly existing contrast and/or brightness changes since involved vectors are zero-mean and normalized. This characteristic clearly support our choice to adopt this criterion for the image alignment problem.

3.1 A Nonlinear Maximization Problem

Since the residual in (4) is based on zero-mean and normalized vectors, it is straightforward to prove that minimizing $E_{ECC}(\mathbf{p})$ is equivalent to maximizing the *enhanced correlation coefficient* (Psarakis and Evangelidis, 2005)

$$\rho(\mathbf{p}) = \hat{\mathbf{i}}_r^t \frac{\bar{\mathbf{i}}_w(\mathbf{p})}{\|\bar{\mathbf{i}}_w(\mathbf{p})\|} \quad (5)$$

where $\hat{\mathbf{i}}_r$ is the normalized reference vector. Notice that even if $\bar{\mathbf{i}}_w(\mathbf{p})$ depends linearly on the parameter vector \mathbf{p} , the resulting objective function is still nonlinear with respect to \mathbf{p} due to the normalization of the warped vector. This of course suggests that its maximization requires nonlinear optimization techniques.

In order to maximize $\rho(\mathbf{p})$ we are going to use a gradient-based iterative approach. More specifically, we are going to replace the original optimization problem by a *sequence* of secondary optimizations. Each such optimization relies on the outcome of its predecessor thus generating a sequence of parameter estimates which hopefully converges to the desired optimizing vector of the original problem. Notice that, at each iteration we do not have to optimize the objective function, but an *approximation* to this function, such that the resulting optimizer are simple to compute. Let us therefore introduce the approximation we intend to apply to our objective function and also derive an analytic expression for the solution that maximizes it.

Suppose that \mathbf{p} is “close” to some nominal parameter vector $\tilde{\mathbf{p}}$ and write $\mathbf{p} = \tilde{\mathbf{p}} + \Delta\mathbf{p}$, where $\Delta\mathbf{p}$ denotes a vector of perturbation. Suppose also that the intensity function I_w and the warping transformation T are of sufficient smoothness to allow for the existence of the required partial derivatives. If we denote as $\tilde{\mathbf{x}}' = T(\mathbf{x}; \tilde{\mathbf{p}})$ the warped coordinates under the nominal parameter vector and $\mathbf{x}' = T(\mathbf{x}; \mathbf{p})$ under the perturbed, then, applying a first order Taylor expansion with respect to the parameters, we can write

$$I_w(\mathbf{x}') \approx I_w(\tilde{\mathbf{x}}') + [\nabla_{\mathbf{x}'} I_w(\tilde{\mathbf{x}}')]^t \frac{\partial T(\mathbf{x}; \tilde{\mathbf{p}})}{\partial \mathbf{p}} \Delta\mathbf{p}, \quad (6)$$

where $\nabla_{\mathbf{x}'} I_w(\tilde{\mathbf{x}}')$ denotes the gradient vector of length 2 of the intensity function $I_w(\mathbf{x}')$ of the warped image evaluated at the nominal coordinates $\tilde{\mathbf{x}}'$ and $\frac{\partial T(\mathbf{x}; \tilde{\mathbf{p}})}{\partial \mathbf{p}}$ the size $2 \times N$ Jacobian matrix of the warp transform with respect to its parameters, evaluated at the nominal values $\tilde{\mathbf{p}}$.

By applying (6) to all points of target area S , forming the linearized version of the warp vector $\bar{\mathbf{i}}_w(\mathbf{p})$ and computing its zero mean counterpart we obtain the following approximation $\rho(\Delta\mathbf{p}|\tilde{\mathbf{p}})$ of the objective

function $\rho(\mathbf{p})$ defined in (5):

$$\rho(\mathbf{p}) \approx \rho(\Delta\mathbf{p}|\tilde{\mathbf{p}}) = \frac{\hat{\mathbf{i}}_r^t \bar{\mathbf{i}}_w + \hat{\mathbf{i}}_r^t \bar{G} \Delta\mathbf{p}}{\sqrt{\|\bar{\mathbf{i}}_w\|^2 + 2\hat{\mathbf{i}}_r^t \bar{G} \Delta\mathbf{p} + \Delta\mathbf{p}^t \bar{G}^t \bar{G} \Delta\mathbf{p}}} \quad (7)$$

where \bar{G} denotes the column-zero-mean counterpart of the size $K \times N$ Jacobian matrix $G(\tilde{\mathbf{p}})$ of the warped intensity vector with respect to the parameters, evaluated at the nominal parameter values $\tilde{\mathbf{p}}$. Note that for notational simplicity, the dependence of the warped vectors on \mathbf{p} has been dropped.

Although $\rho(\Delta\mathbf{p}|\tilde{\mathbf{p}})$ is a non-linear function of $\Delta\mathbf{p}$, its maximization results in a closed-form solution. This solution is given, without proof, by the next theorem (Evangelidis and Psarakis, 2007).

Theorem 1: Consider the objective function defined in (7) and the orthogonal projection matrix $P_G = \bar{G}(\bar{G}^t \bar{G})^{-1} \bar{G}^t$ of size K . Then, as far as the maximal value of $\rho(\Delta\mathbf{p}|\tilde{\mathbf{p}})$ is concerned, we distinguish the following two cases: Case $\hat{\mathbf{i}}_r^t \bar{\mathbf{i}}_w > \hat{\mathbf{i}}_r^t P_G \bar{\mathbf{i}}_w$: here we have a maximum, specifically

$$\max_{\Delta\mathbf{p}} \rho(\Delta\mathbf{p}|\tilde{\mathbf{p}}) = \sqrt{\frac{(\hat{\mathbf{i}}_r^t \bar{\mathbf{i}}_w - \hat{\mathbf{i}}_r^t P_G \bar{\mathbf{i}}_w)^2}{\|\bar{\mathbf{i}}_w\|^2 - \hat{\mathbf{i}}_r^t P_G \bar{\mathbf{i}}_w}} + \hat{\mathbf{i}}_r^t P_G \hat{\mathbf{i}}_r, \quad (8)$$

which is attainable for the following optimal perturbation

$$\Delta\mathbf{p}^o = (\bar{G}^t \bar{G})^{-1} \bar{G}^t \left\{ \frac{\|\bar{\mathbf{i}}_w\|^2 - \hat{\mathbf{i}}_r^t P_G \bar{\mathbf{i}}_w}{\hat{\mathbf{i}}_r^t \bar{\mathbf{i}}_w - \hat{\mathbf{i}}_r^t P_G \bar{\mathbf{i}}_w} \hat{\mathbf{i}}_r - \bar{\mathbf{i}}_w \right\}. \quad (9)$$

Case $\hat{\mathbf{i}}_r^t \bar{\mathbf{i}}_w \leq \hat{\mathbf{i}}_r^t P_G \bar{\mathbf{i}}_w$: here we have a supremum, specifically

$$\sup_{\Delta\mathbf{p}} \rho(\Delta\mathbf{p}|\tilde{\mathbf{p}}) = \sqrt{\hat{\mathbf{i}}_r^t P_G \hat{\mathbf{i}}_r}, \quad (10)$$

which can be approached arbitrarily close by selecting

$$\Delta\mathbf{p}^o = (\bar{G}^t \bar{G})^{-1} \bar{G}^t \{ \lambda \hat{\mathbf{i}}_r - \bar{\mathbf{i}}_w \}, \quad (11)$$

with λ a positive scalar, of sufficiently large value.

In order to be able to use the results of *Theorem 1* the positive quantity λ must be defined. It is clear that λ must be selected so that the resulting $\rho(\Delta\mathbf{p}^o|\tilde{\mathbf{p}})$ satisfies $\rho(\Delta\mathbf{p}^o|\tilde{\mathbf{p}}) > \rho(0|\tilde{\mathbf{p}})$ and $\rho(\Delta\mathbf{p}^o|\tilde{\mathbf{p}}) \geq 0$. Possible values of λ provide the following lemma (Evangelidis and Psarakis, 2007).

Lemma 1: Let $\hat{\mathbf{i}}_r^t \bar{\mathbf{i}}_w \leq \hat{\mathbf{i}}_r^t P_G \bar{\mathbf{i}}_w$ and define the following two values for λ

$$\lambda_1 = \sqrt{\frac{\hat{\mathbf{i}}_r^t P_G \bar{\mathbf{i}}_w}{\hat{\mathbf{i}}_r^t P_G \hat{\mathbf{i}}_r}}, \quad \lambda_2 = \frac{\hat{\mathbf{i}}_r^t P_G \bar{\mathbf{i}}_w - \hat{\mathbf{i}}_r^t \bar{\mathbf{i}}_w}{\hat{\mathbf{i}}_r^t P_G \hat{\mathbf{i}}_r}. \quad (12)$$

Then for $\lambda \geq \lambda_1$ we have that $\rho(\Delta\mathbf{p}^o|\tilde{\mathbf{p}}) > \rho(0|\tilde{\mathbf{p}})$; for $\lambda \geq \lambda_2$ that $\rho(\Delta\mathbf{p}^o|\tilde{\mathbf{p}}) \geq 0$; finally for $\lambda \geq \max\{\lambda_1, \lambda_2\}$ we have both inequalities valid.

Let us now translate the above results into an *i-iterative* scheme in order to obtain the solution to the original nonlinear optimization problem. To this end, let us assume that from iteration $j - 1$ we have available the parameter estimate \mathbf{p}_{j-1} and we adopt the following additive rule

$$\mathbf{p}_j = \mathbf{p}_{j-1} + \Delta\mathbf{p}_j. \quad (13)$$

Then, using \mathbf{p}_{j-1} we can compute $\bar{\mathbf{i}}_w(\mathbf{p}_{j-1})$ and $\bar{G}(\mathbf{p}_{j-1})$ and optimize the approximation $\rho(\Delta\mathbf{p}_j|\mathbf{p}_{j-1})$ with respect to $\Delta\mathbf{p}_j$. The iterative algorithm is summarized below.

Initialization

- Use I_r to compute $\hat{\mathbf{i}}_r$ defined in (3).
- Initialize \mathbf{p}_0 and set $j = 1$.

Iteration Steps

- Using $T(\mathbf{x}; \mathbf{p}_{j-1})$ warp I_w and compute $\bar{\mathbf{i}}_w(\mathbf{p}_{j-1})$
- Using $T(\mathbf{x}; \mathbf{p}_{j-1})$ warp the gradient ∇I_w of I_w and compute the Jacobian matrix $\bar{G}(\mathbf{p}_{j-1})$
- Compare $\hat{\mathbf{i}}_r \bar{\mathbf{i}}_w$ with $\hat{\mathbf{i}}_r P_G \bar{\mathbf{i}}_w$ and compute perturbations $\Delta\mathbf{p}_j^o$ either from (9) or using (11) and (12)
- Update parameter vector $\mathbf{p}_j = \mathbf{p}_{j-1} + \Delta\mathbf{p}_j^o$.

If $\|\Delta\mathbf{p}_j^o\| \geq \varepsilon_p$ then, $j++$ and repeat; else stop.

As it is indicated above, the algorithm is executed until the norm of the perturbation vector $\|\Delta\mathbf{p}_j^o\|$ becomes smaller than a predefined threshold ε_p .

We must stress at this point that the convergence of the proposed algorithm can critically be affected by the values of vector \mathbf{p}_0 when the images overlap by a small amount or one image is only a small deformed subset of the other. In such cases appropriate values of vector \mathbf{p}_0 should prevent the algorithm to be trapped into local maxima. Such a reliable estimation for the initialization of the algorithm can be obtained by using a correlation based search method (Shum and Szeliski, 2000) or a landmark-based method (Johnson and Christensen, 2002). However, in this paper we consider that the images overlap by a large amount thus excluding such cases.

Concluding, the structure of the iterative algorithm is very similar to the forward additive scheme of the Lucas-Kanade (LK) algorithm (Lucas and Kanade, 1981), one of the most frequently used algorithm for the image alignment problem, but as we are going to see in the next section, the proposed updating scheme improves the performance significantly.

3.2 Parametric Models

In this work, to model the warping process we are going to use the following eight-parameters projective

transformation (homography)

$$\bar{\mathbf{x}}' = T(\bar{\mathbf{x}}; \mathbf{p}) = \frac{1}{P} \begin{bmatrix} p_1 & p_2 & p_3 \\ p_4 & p_5 & p_6 \end{bmatrix} \begin{bmatrix} \mathbf{x} \\ 1 \end{bmatrix} \quad (14)$$

where $P = p_7x + p_8y + 1$. This class of transformations is the most general class of the well known 2-D planar motion models that gives the exact number of desired parameters to account for all the possible camera motions.

For the Jacobian of the projective model we have

$$\frac{\partial T(\bar{\mathbf{x}}; \mathbf{p})}{\partial \mathbf{p}} = \frac{1}{P} \begin{bmatrix} x & y & 1 & 0 & 0 & 0 & -x'x & -x'y \\ 0 & 0 & 0 & x & y & 1 & -y'x & -y'y \end{bmatrix}, \quad (15)$$

where x', y' are the elements of vector $\bar{\mathbf{x}}'$.

As it is clear from (14), eight-parameters projective transformation is a nonlinear function of its parameters and its stability as well as the continuity of its Jacobian are depended on the values of the denominator P . To ensure its stability and the existence of its Jacobian, we restrict ourselves on admissible (Radke et al., 2000) estimations of the transform. Note also that in spite of the affine model which has a Jacobian that does not depend on the warping parameters, projective model, as it is obvious from (15), has a Jacobian that depends on the parameters \mathbf{p} and thus it must be updated on each iteration of the iterative algorithms. Several approximations of projective transformation such as bilinear and polynomial can be used in order to partially overcome these problems. Note though that by following such an approach, the strong deformations introduced by the projective transformation cannot be exactly adjusted and this may lead to meaningless alignment results.

4 SIMULATION RESULTS

In this section we are going to evaluate our algorithm and compared it against the forward additive version of the Lucas-Kanade algorithm (Lucas and Kanade, 1981), as it is implemented in (Baker and Matthews, 2004). As we have already mentioned, we perform two sets of experiments. In both sets, for the modelling of the warping process the nonlinear projective transformation defined in (14) is used, but in the first set of experiments the reference image profiles are created using a nonlinear projective transformation, while in the second set by using an affine one. We must stress at this point that for all aspects affecting the simulation experiments, we made an effort to stay exactly within the frame specified in (Baker and Matthews, 2004). Before we present our results we give some details for the experimental setup as

well as the figures of merit we are going to use in order to fairly compare the competing algorithms.

4.1 Experimental Setup

The experimental setup is described analytically in (Baker and Matthews, 2004). In brief, we have an input image I_0 and we crop a rectangular area of the image. By adding an appropriate translation in the coordinates of the points corresponding to the corners of the cropped image and adding Gaussian noise with standard deviation σ_p we perturb them. The four initial points, and their warped versions defines the parameter vector of the projective transformation. Using these values, we map all target points and warp I_0 to create a reference image I_r . The competing algorithms then are applied for the alignment of I_r with I_0 . In order to create a reference image I_r in the second set of our experiments, we follow a similar procedure. Note though that in this case we select three points instead of four, from the rectangular cropped area (i.e. top left and right corner and bottom middle point) and use them in order to define the six parameters of the affine transform.

In order to measure the quality of the estimated parameters we use the Mean Square Distance (MSD) between the exact warped version of the four (three) points and their estimated counterparts. More formally, if we denote as \mathbf{p}_r the parameter vector which we use in defining the reference profile I_r , \mathbf{p}_j the current estimation of the corresponding algorithm at j -th iteration and C the set of the four(three) above mentioned points, we use the mean of the following sequence

$$e(j) = \frac{1}{8(6)} \sum_{\mathbf{x} \in C} \|T(\mathbf{x}; \mathbf{p}_r) - T(\mathbf{x}; \mathbf{p}_j)\|^2. \quad (16)$$

Each element of the mean sequence (i.e. for a specific value of iteration index j) is obtained by averaging over a large number of image pairs that differ in the noise realization, and captures the learning ability of the algorithms (average rate of convergence (Baker and Matthews, 2004)). However, in order to not present biased results, we compute the above mentioned mean sequence for those realizations where both algorithms have converged. The convergence criterion is that the square distance $e(j)$ at a prescribed maximal iteration j_{max} is below a certain threshold T_{MSD} , that is $e(j_{max}) \leq T_{MSD}$.

As a second figure of merit we use the percentage of converging (PoC) runs (frequency of convergence (Baker and Matthews, 2004)). This quantity is the percentage of runs that converge up to maximal iteration j_{max} , based again on the above mentioned convergence criterion. PoC is depicted as a function of

the point deviation σ_p , the most important factor that affects the performance of both algorithms.

Since it is natural to prefer an algorithm that converges quickly with high probability, we propose a third figure of merit that captures exactly this point (Evangelidis and Psarakis, 2007). In other words we propose the generation of a histogram depicting the probability of successful convergence at each iteration. Specifically a run of an algorithm on an image pair realization will be considered as having converged at iteration n when the squared error $e(j)$ goes below the threshold T_{MSD} for the first time at iteration $j = n$. It is clear that we prefer a histogram to be concentrated over mostly small iteration-numbers.

In all experiments that follow we use $T_{MSD} = 1 \text{ pixel}^2$.

4.2 Minimal Case

In this subsection we present the results we obtained from the first set of experiments we have conducted. As it is above described, in this case we create the reference profile by using a projective transform and we model the warping process by using a transformation of the same class.

4.2.1 Experiment I

In the first experiment, the alignment algorithms try to compensate only the geometric distortions since this is the only that has been applied to images. Specifically, we use the ‘‘Takeo’’ image (Baker and Matthews, 2004) as input image and we create 500 different reference profiles for each integer values of σ_p in the range $[1, 10]$. For each one of the 500 realizations, we permit the algorithms to make 15 iterations ($j_{max} = 15$). Since no intensity noise or photometric distortion is applied to image, we expect MSD to reach very low levels which cannot be zero due to finite precision arithmetic.

Figure 1 depicts the relative performance of the two algorithms. As we mentioned above, we present the arithmetic mean of the sequence $e(j)$ for those realizations where both algorithms have converged. Three cases are investigated; (a) $\sigma_p = 2$, (b) $\sigma_p = 6$ and (c) $\sigma_p = 10$. In all these cases our algorithm exhibits a significantly smaller MSD which is order(s) of magnitude better than the one obtained by the LK scheme. Furthermore concerning the PoC, as we can see from Figure 1.(d), our algorithm exhibits better performance for all values of σ_p . Specifically for strong deformations ($\sigma_p = 10$) the improvement can become quite significant (18%). As far as the probability of successful convergence is concerned, we applied the algorithms for a maximal number of 100 iterations ($j_{max} = 100$). In Figure 2 the resulting graphs

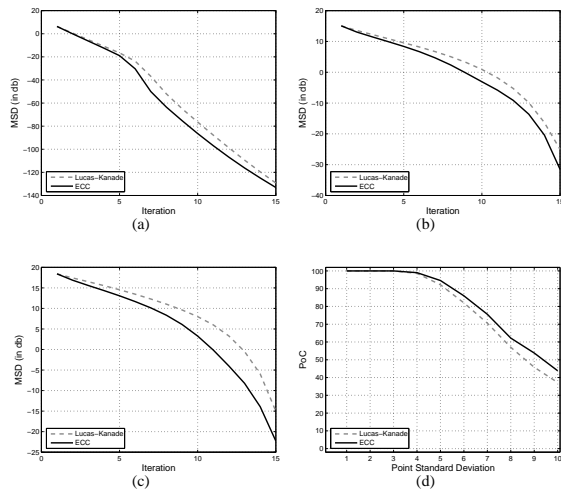


Figure 1: MSD in dB as a function of number of iterations; (a) $\sigma_p = 2$, (b) $\sigma_p = 6$, (c) $\sigma_p = 10$. In (d), PoC as a function of σ_p for $j_{max} = 15$.

for the cases of $\sigma_p = 6$ and $\sigma_p = 10$ are shown. In order however, for the differences to become visible, we present only the first 50 bins of the histogram. As we can clearly see the proposed algorithm has larger percentage of converged realizations in smaller iteration numbers than the LK scheme.

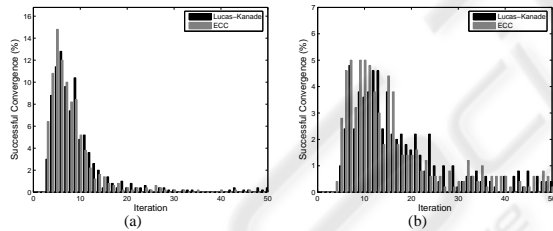


Figure 2: Histograms of successful convergence as a function of number of iterations; (a) $\sigma_p = 6$, (b) $\sigma_p = 10$.

4.2.2 Experiment II

In this experiment we repeat the previous procedure, but we add now intensity noise to both images before their alignment. Specifically, the standard deviation of the noise we add into the images is equal to 8 gray levels. Due to this noise, even theoretically the MSD can no longer be equal to 0.

In Figure 3 the results we obtained are shown. For the case of $\sigma_p = 2$ we observe that both algorithms reach an MSD floor value, while in the other two cases this is not visible. Note though that the proposed algorithm outperforms the LK scheme by a half or a full order of magnitude. Furthermore, the proposed algo-

rithm exhibits a larger PoC score confirming thus its superiority. Regarding the histograms, as we can see

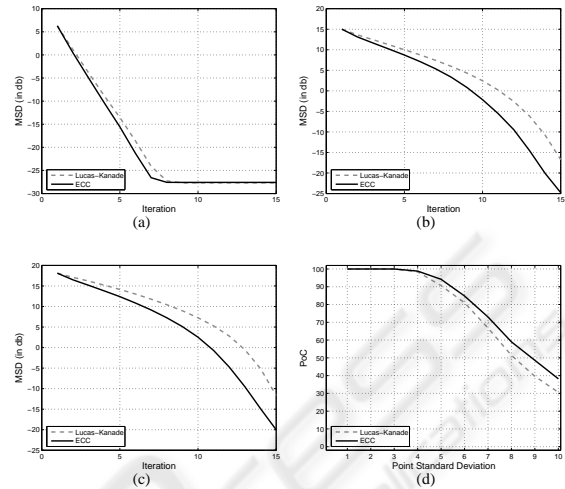


Figure 3: MSD in dB as a function of number of iterations for the noisy (8 gray levels) “Takeo” image; (a) $\sigma_p = 2$, (b) $\sigma_p = 6$, (c) $\sigma_p = 10$. In (d), PoC as a function of σ_p for $j_{max} = 15$.

from Figure 4, the resulting histograms are very similar to the previous noise-free case with the histograms of the proposed algorithm having a larger percentage of converged realizations in smaller iteration numbers than the LK scheme.

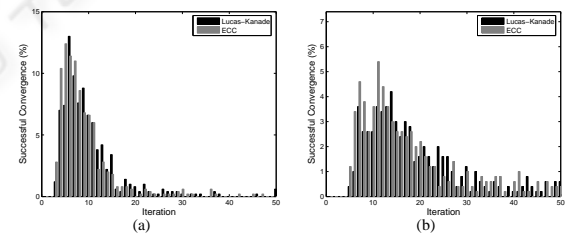


Figure 4: Histograms of successful convergence as a function of number of iterations for the noisy (8 gray levels) “Takeo” image; (a) $\sigma_p = 6$, (b) $\sigma_p = 10$.

4.3 Over-Modelling Case

In this subsection we examine the behavior of the algorithms under the influence of over-modelling. Specifically, we create the reference profiles by using an affine transform, but we still model the warping process by using a nonlinear projective transformation. Since six parameters are required for the affine transform, the values of two more parameters (p_7, p_8) must be estimated by the alignment algorithms. Ideally these values must be equals to zero. Since we like

to evaluate the performance of the algorithms under the influence of the over-modelling, we concentrate ourselves on the realizations where both algorithms are converged when the warping process is modelled by an affine transformation. Then, we run the competing algorithms on these common converged realizations, the converged realizations for each one in the over-modelling case are counted, and the resulting learning curves and PoC scores are presented. As far as the probability of convergence is concerned, as in the minimal case we applied the algorithms for a maximum of 100 iterations and the resulting histograms are also presented. For comparison purposes, the learning curves as well as PoC scores obtained from the affine modelling are superimposed on the corresponding plots. As in the previous subsection two experiments are conducted.

4.3.1 Experiment III

This experiment is very similar to Experiment I. As we already mentioned, the basic difference is that the reference profiles have been created by using affine transformations instead of projective ones. As it was

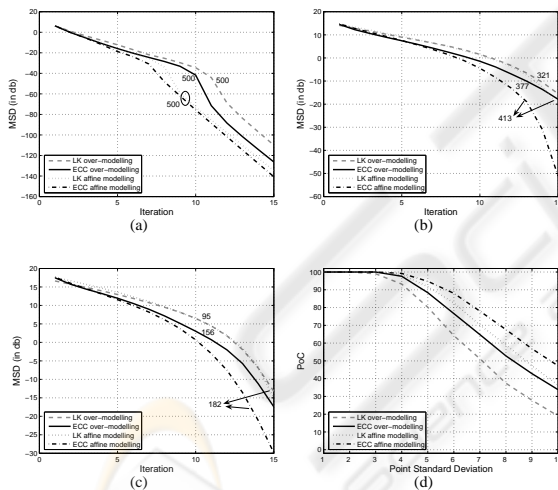


Figure 5: Over-modelling case. MSD in dB as a function of number of iterations; (a) $\sigma_p = 2$, (b) $\sigma_p = 6$, (c) $\sigma_p = 10$. In (d), PoC as a function of σ_p for $j_{\max} = 15$.

expected (Figure 5), over-modelling degrades the performance of the estimation, affects PoC score as well as the learning ability of the algorithms. However, we observe that ECC algorithm seems to be more robust in the over-modelling case than the LK algorithm. Indeed, this is exactly the case if we take into account the number of realizations in which each algorithm has converged (the values appeared next to each curve). For example, for the case of $\sigma_p = 10$ (Figure 5.(c)), in a total of 182 common “success-

fully” converged realizations under affine modelling (Evangelidis and Psarakis, 2007), LK algorithm succeeded in aligning 95 profiles (52%), while ECC algorithm 156 (86%). Figure 5.(d) depicts the algorithms PoC as a function of σ_p for both cases. We observe that the behavior of ECC algorithm is better as compared to the LK scheme which exhibits a significant degradation in its performance due to over-modelling. In Figure 6 the obtained histograms are shown. As we can see from Figure 6 the histograms resulting from the proposed algorithm are more concentrated over smaller iteration numbers than the histograms resulting from the LK scheme. This is more evident in Figure 6.(b) where the resulting histogram from the LK scheme is almost uniformly spread over the range 5 to 30.

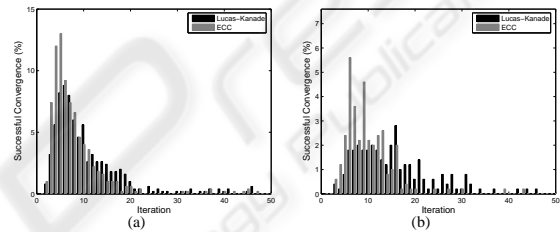


Figure 6: Over-modelling case. Histograms of successful convergence as a function of number of iterations; (a) $\sigma_p = 6$, (b) $\sigma_p = 10$.

4.3.2 Experiment IV

The conditions of this experiment are similar to the conditions of Experiments III, except the fact that we try to align noisy images, where the standard deviation of the additive noise is 8 gray levels. The obtained simulation results are shown in Figure 7. As in the previous experiments, ECC algorithm seems to outperform the LK scheme. As we can see from the corresponding figures, ECC based algorithm has converged in more realizations than LK algorithm has. It is also worth noting from Figure 7.(d) where the PoC score is depicted, that the performance of ECC algorithm in the over-modelling case almost coincides with the performance of LK algorithm in the case of affine modelling. Finally, similar conclusion with that of the previous experiment can be drawn from Figure 8 where the obtained histograms with the percentages of successful convergence are depicted.

5 CONCLUSIONS

In this paper a recently proposed parametric alignment algorithm was used in the projective image re-

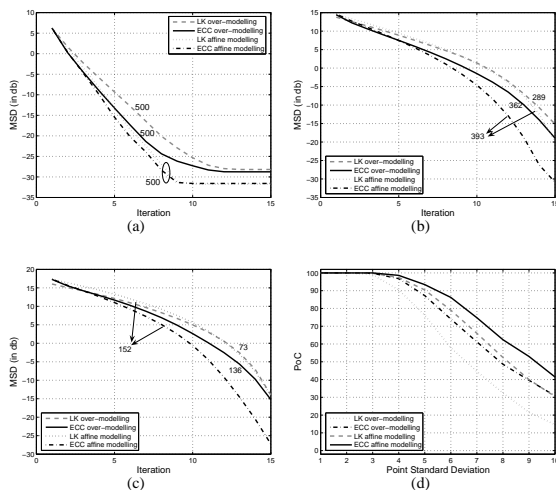


Figure 7: Over-Modelling case. MSD in dB as a function of number of iterations for the noisy (8 gray levels) “Takeo” image; (a) $\sigma_p = 2$, (b) $\sigma_p = 6$, (c) $\sigma_p = 10$. In (d), PoC as a function of σ_p for $j_{max} = 15$.

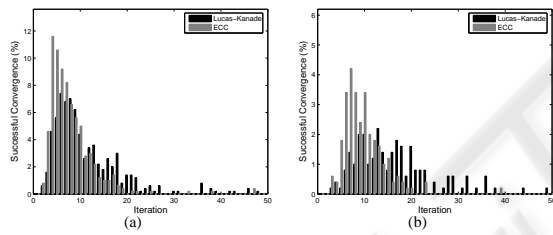


Figure 8: Over-Modelling case. Histograms of successful convergence as a function of number of iterations for the noisy (8 gray levels) “Takeo” image; (a) $\sigma_p = 6$, (b) $\sigma_p = 10$.

gistration problem. This algorithm aims at maximizing the Enhanced Correlation Coefficient function which is a robust similarity measure against both geometric and photometric distortions. The optimal parameters are obtained by iteratively solving, a sequence of approximate nonlinear optimization problems, which enjoy a simple closed-form solution with low computational cost. The algorithm was compared against the well known Lucas-Kanade algorithm, through numerous simulation examples involving ideal and noisy conditions, strong and weak geometric deformations and even over-modelling of the warping transformation. In all cases the proposed algorithm exhibited a better behavior with an improvement in speed, as well as in probability of convergence as compared to the Lucas-Kanade algorithm.

ACKNOWLEDGEMENTS

This work was supported by the General Secretariat for Research and Technology of Greek Government as part of the project “XROMA”, PENED 01.

REFERENCES

- Anandan, P. (1989). A computational framework and an algorithm for the measurement of visual motion. *International Journal of Computer Vision*, 2(3):283–310.
- Baker, S. and Matthews, I. (2004). Lucas-kanade 20 years on: A unifying framework: Part 1: The quantity approximated, the warp update rule, and the gradient descent approximation. volume 56, pages 221–255.
- Evangelidis, G. D. and Psarakis, E. Z. (2007). Parametric image alignment using enhanced correlation coefficient maximization. *Submitted to IEEE Trans. on PAMI, submission TPAMI-0026-0107*.
- Fuh, C. and Maragos, P. (1991). Motion displacement estimation using an affine model for image matching. *Optical Engineering*, 30(7):881–887.
- Gleicher, M. (1997). Projective registration with difference decomposition. In *Proc. of IEEE International Conference on Computer Vision and Pattern Recognition (CVPR’97)*. San Juan, Puerto Rico.
- Hager, G. D. and Belhumeur, P. N. (1998). Efficient region tracking with parametric models of geometry and illumination. *IEEE Trans. on PAMI*, 20(10):1025–1039.
- Johnson, H. and Christensen, G. (2002). Consistent landmark and intensity-based image registration. *IEEE Transactions on Medical Imaging*, 21(5):450–461.
- Lucas, B. D. and Kanade, T. (1981). An iterative image registration technique with an application to stereo vision. In *Proc. of 7th International Joint Conf on Artificial Intelligence (IJCAI)*. Vancouver, British Columbia.
- Psarakis, E. Z. and Evangelidis, G. D. (2005). An enhanced correlation-based method for stereo correspondence with sub-pixel accuracy. In *Proc. of 10th IEEE International Conference on Computer Vision (ICCV 2005)*. Beijing, China.
- Radke, R., Ramadge, P., Echigo, T., and Iisaku, S. (2000). Efficiently estimating projective transformations. In *Proc. of IEEE International Conference on Image Processing (ICIP’00)*, pages 232–235. Vancouver, Canada.
- Shum, H. and Szeliski, R. (2000). Construction of panoramic image mosaics with global and local alignment. *International Journal on Computer Vision*, 36(2):101–130.
- Szeliski, R. (2005). *Handbook of Mathematical Models of Computer Vision*. Springer. ch. 17.
- Szeliski, R. (2006). Image alignment and stitching: A tutorial. *Foundations and Trends in Computer Graphics and Computer Vision*, 2(1):1–104.